A deuterium/hydrogen Lyman alpha absorption cell photometer developed for the Nozomi spacecraft

Tôhoku Geophys. Journ. (Sci. Rep. Tôhoku Univ., Ser. 5), Vol. 37, No. 2, pp. 109-123, 2006

A Deuterium/Hydrogen Lyman Alpha Absorption Cell Photometer Developed for the Nozomi Spacecraft

YUICHI ITO[1] and HIROSHI FUKUNISHI[2]

(Received August 24, 2006; Accepted August 29, 2006)

Abstract: A deuterium/hydrogen Lyman α absorption cell photometer has been developed for the Nozomi spacecraft which is the Japanese first planetary spacecraft to Mars. This photometer aims to observe the Martian hydrogen and deuterium corona and their D/H ratio. Unfortunately, the Nozomi spacecraft project ended in failure by engine and telemeter trouble during the insertion phase to Mars in December 2003. In this paper, we summarize the performance of the developed D/H absorption cell photometer and the results of simulation studies on D/H ratio retrieval from Martian corona measurement.

1 Introduction

There is no evidence on the existence of massive liquid water in the present climate system of Mars. However, from the geological features of massive water flows on the Martian surface, it is suggested that Mars had enough water to form a global layer 500 m thick or greater in the past (Carr, 1979, 1986, 1987, 1990). One of the water loss mechanism is generally thought to be atmospheric escape to space via the Martian exosphere (Chamberlain, 1969; Fox, 1993; Hunten, 1982, 1990; Liu *et al.*, 1976; Visconti, 1977; Zahnle, 1986). Deuterium atoms which have chemically the same characteristics as hydrogen atoms but twice mass condensate through these processes. Therefore, the atmospheric D/H ratio increases in the evolutionary history of the Martian atmosphere. The detection of the D/H ratio has been challenged despite of its difficulty.

The first attempt of D/H ratio measurement was performed by Owen *et al.* (1988). They had measured the emission ratio of the water molecular band in the Martian lower atmosphere using the 3.6-m infrared telescope with a Fourier transform spectrometer at Mauna Kea, Hawaii. They reported a D/H ratio of $9\pm4\times10^{-4}$ from the emission intensities of HDO and H_2O. Bjoraker (1989) also performed similar spectroscopic observations at Kuiper Airborne observatory and obtained a D/H ratio of $7.8\pm0.3\times10^{-4}$. Later, the Phobos spacecraft performed a solar occultation observation of HDO and H_2O absorption using the Augustine infrared spectrometer (Korablev *et al.*, 1993). However, only the upper limit of the D/H ratio was obtained as 5.0×10^{-4} within a statistical uncertainty of the detection. Analysis of the SNC (Shergottites, Nakhlites and Chassin-

[1] Max-Planck-Institut für Sonnensystemforschung, Max-Planck-Straße 2, 37191, Katlenburg-Lindau, Germany.
[2] Department of Geophysics, Graduate School of Science, Tohoku University, Aramaki-Aoba, Sendai 980-8578, Japan.

gnites) meteorites which are thought to have come from the surface of Mars also provided information of the Martian D/H ratio as $8.1 \pm 0.3 \times 10^{-4}$ on the Martian surface (Watson, 1993). Krasnopolsky *et al.* (1998) detected deuterium Lyman α line using the Hubble space telescope. They reported that the deuterium Lyman α intensity is a 23 ± 6 Rayleighs at the limb of Mars. Corresponding HD/H_2 ratio of the upper atmosphere is a factor of 11 times smaller than that of the ratio of HDO and H_2O of the lower atmosphere.

The discrepancy in the vertical direction urged the construction of photochemical models, thereby enhanced the knowledge of the hydrated and deuterized compounds. Yung *et al.* (1988) first constructed a photochemical model including deuterized compounds which had become a standard model later. They defined the partitioning index ($R=(HD/H_2)/(HDO/H_2O)$) to generalize the formation rate of the deuterized compounds in the air. They estimated a value of $R=1.6$ under an assumption that H_2 and HD can not be controlled only by the isotopic exchange $HD+H_2O \Leftrightarrow HDO+H_2$ on the thermal equilibrium condition. However, Krasnopolsky's observations (Krasnopolsky, 1998) denied the model result ($R=0.09$). Extensive efforts were paid to the depletion mechanism of the deuterium in the vertical direction because such investigations give the upper limit of escape. It was pointed out that there is either an unknown loss mechanism to reduce the partitioning index or a catalyst to increase the efficiency of the isotopic reaction (Yung *et al.*, 1998). Several plausible mechanisms have been proposed so far.

Fouchet *et al.* (2000) applied the isotopic condensation effect at the hygropause. Cheng *et al.* (1999) constructed a photo-induced fractionation effect (PHIFE) theory. They applied to the vertical depletion of the deuterium on the Martian corona and explained a factor of 2.5. Bertaux *et al.* (2001) discussed a combination of the photo-induced fractional effect (PHEFE) and the condensation/evaporation fractional effect (CEFE) which can produce a cold trap for deuterium in the atmosphere of Mars. The recent model (Bertaux *et al.*, 2001) gives a reasonable explanation by a factor of 9.5 difference of the D/H ratio with an estimation of smaller quantity of the water.

Novel findings and scientific achievements on the D/H ratio in the past two decades are summarized as follows. (1) Low D/H ratio in the upper atmosphere (Krasnopolsky *et al.*, 1998); comparatively high condensation of HDO/H_2O ratio in the lower atmosphere (Owen *et al.*, 1998; Bjoraker., 1989); high D/H ratio in the SNC meteorite (Watson *et al.*, 1993) on the Martian surface. (2) Successful development of a photochemical model to explain the discrepancy of the discrete D/H ratio value at altitudes of 3-levels (Bertaux *et al.*, 2001) with an affirmative implication of under ground water (Krasnopolsky *et al.*, 1998; Krasnopolsky, 2000).

The Nozomi spacecraft is the Japanese first planetary mission to Mars. The main target of Nozomi is to investigate the interaction processes between the Martian upper atmosphere and the solar wind with 14 scientific instruments (Tsuruda *et al.*, 1996). One of these instruments is an ultraviolet imaging spectrometer which consists of a D/H absorption cell photometer (UVS-P) as shown in Fig. 1 and a grating spectrometer (UVS-G) (Fukunishi *et al.*, 1999; Taguchi *et al.*, 2000a, 2000b). As Mars has no intrinsic

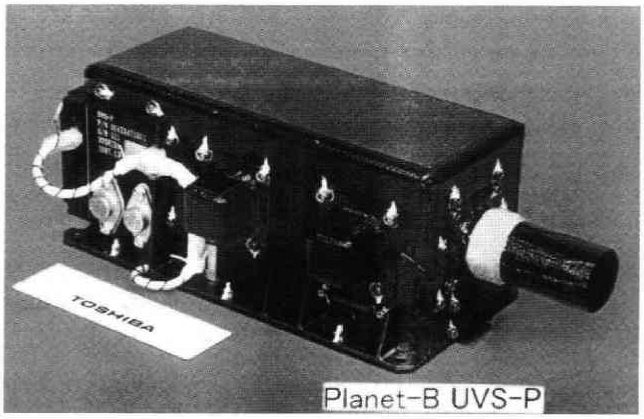

Fig. 1. View of the hydrogen and deuterium absorption cell photometer (UVS-P). The UVS-P consists of a solar blind type photomultiplier and hydrogen and deuterium absorption cells. The weight of UVS-P is 0.6 kg.

magnetic field, it is generally believed that the solar wind interacts directly with the Martian upper atmosphere so that the upper atmosphere environment is strongly controlled by solar activity. The UVS-P is applied to imaging observations of the Martian deuterium corona as well as the hydrogen corona. Collaborated observations have been proposed among Nozomi and several missions of NASA and ESA. However, the Nozomi spacecraft was abandoned by engine and telemeter trouble during the insertion phase to Mars in December 2003, and this project ended in failure. However, similar projects of D/H ratio measurement using the absorption cells (Esposito *et al.*, 1998) at the Cassini mission as well as the PFS (Planetary Fourier transform Spectrometer) of the Mars Express mission (Formisano *et al.*, 2002) encourage us to report our work. In this paper, we summarize the performance of the developed D/H absorption cell photometer and the results of simulation studies on D/H ratio retrieval from Martian corona measurement.

2 Development of the D/H absorption cell photometer

The UVS-P is a solar blind type Lyman α photometer with deuterium and hydrogen absorption cells, which enables us to obtain information on (1) the kinetic temperature of hydrogen Lyman α emission and (2) the D/H ratio of Lyman α emissions.

2.1 Principle of the absorption cell photometer

The principle of detecting the kinetic temperature of hydrogen is to utilize the transmission property of the absorption cell, which can be mathematically expressed as the convolution of the incident emission and the absorption cell profile. Hydrogen molecules never absorb the Lyman α emission at static condition. However, by activating the filaments inside the cells, thermally dissociated hydrogen (or deuterium) atoms are generated. Then the generated hydrogen (deuterium) atoms resonantly scatter

incident Lyman α emission. Since resonantly scattered photons are re-directed omni-directionally, the photons except for those in the direction of the optical axis cannot reach the detector. Consequently, the absorption cell works as a narrow-width negative optical filter which exclusively absorbs the Lyman α emission. By controlling the electric current of the filaments inside the cell, the absorption cell profiles is controlled. The transmittance of the cell, $T(\lambda)$, is given as a function of wavelength λ as

$$T(\lambda)=\exp(-\tau(\lambda)) \tag{1}$$

where τ is the optical thickness of hydrogen atoms given by

$$\tau=n_H\cdot\sigma(\lambda)\cdot L \tag{2}$$

and n_H is the hydrogen atom density produced by dissociation of hydrogen molecules inside the cell, L is the optical path along the cell, and $\sigma(\lambda)$ is the absorption cross section of the hydrogen Lyman α line. The absorption cross section $\sigma(\lambda)$ is expressed as a Gaussian function as

$$\sigma(\lambda)=\sigma_0\cdot\exp\left[-\left(\frac{\Delta\lambda}{\lambda_c}\right)^2\right] \tag{3}$$

where $\Delta\lambda=\lambda-\lambda_0$ is the difference of wave length from the line center, and

$$\lambda_c=\frac{\lambda}{c}\cdot\left(\frac{2kT_{atom}}{m_H}\right)^{\frac{1}{2}} \tag{4}$$

Furthermore, σ_0 (cm^2) is the absorption cross section at the line center, expressed as

$$\sigma_0=\frac{\sqrt{\pi}e^2}{m_e c}\cdot\lambda_0\cdot\left(\frac{m_H}{2kT_{atom}}\right)^{\frac{1}{2}}\cdot f \tag{5}$$

In equation (5), index f is the oscillator strength, which represents the degree of scattering, 0.4164 for hydrogen and 0.4165 for deuterium. Furthermore, m_e (g) is the mass of electron, e (C) is the charge of electron, c is the light velocity, k is the Boltzman constant, m_H (g) is the mass of hydrogen atom, and T_{atom} (K) is the atomic hydrogen gas temperature. The source line spectrum of hydrogen Lyman α emission is expressed as a Gaussian form, which is given by

$$S(\lambda)=S_0\cdot\exp\left[-\left(\frac{\Delta\lambda}{\lambda_s}\right)^2\right] \tag{6}$$

where

$$\lambda_s=\frac{\lambda}{c}\cdot\left(\frac{2kT_s}{m_H}\right)^{\frac{1}{2}} \tag{7}$$

In equation (7), T_s is the kinetic temperature of an incident Lyman α emission source. The incident Lyman α emission transmitted through the absorption cell changes its spectrum form, and has a normalized profile as

$$G(\lambda)=\frac{S(\lambda)\cdot T(\lambda)}{S_0}=S_n(\lambda)\cdot T(\lambda) \tag{8}$$

where $S_n(\lambda)$ is the normalized spectrum of the incident light. The wavelength integrated transmission ratio, TRN, is given as

$$TRN=\frac{\int_{-\infty}^{\infty} S(\lambda)\cdot T(\lambda)\, d\lambda}{\int_{-\infty}^{\infty} S_n(\lambda) d\lambda} \tag{9}$$

From (9), the transmission ratio can be determined by 4 parameters: (1) temperature of the incident Lyman α emission source, (2) Doppler shift of the incident Lyman α line center from the line center of the cell absorption profile due to the relative motion of spacecraft, (3) optical depth of the absorption cell, and (4) temperature of hydrogen atoms inside the cell. In case that the absorption cell is accurately calibrated, it is possible to estimate the kinetic temperature of the incident Lyman α emission.

2.2 Principle of the D/H ratio measurement using the absorption cell photometer

By combining the hydrogen and deuterium absorption cells, the emission rate of deuterium to hydrogen Lyman α can be also detected, where these utilize the absoluteness of the Lyman α emission lines and the transmittance of the absorption cells. The absorption cell photometer is modeled as shown in Fig. 2. Then the model can be formulated as follows.

$$T_{H1}\cdot C_H + T_{D1}\cdot C_D + B_G = S_1 \tag{10}$$

$$T_{H2}\cdot C_H + T_{D2}\cdot C_D + B_G = S_2 \tag{11}$$

where T_{H1}, T_{H2} (T_{D1}, T_{D2}) denote the transmission of the hydrogen (deuterium) at each operation mode: 1 and 2. C_H and C_D denote the hydrogen and deuterium Lyman α intensities, respectively. B_G denotes background light including dark noise. Here, B_G term is omitted under an assumption of no background light, thereby the equations can

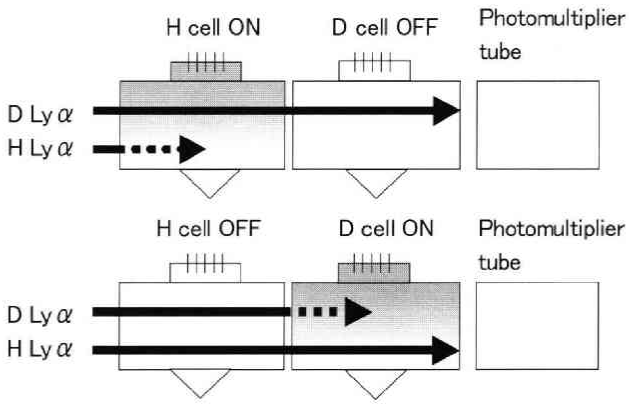

Fig. 2. Schematic diagram of the D/H absorption cell photometer. The hydrogen and deuterium Lyman α emissions are separately detected by changing the transmission of the deuterium or hydrogen absorption cell.

be solved by matrix inversion as

$$\begin{bmatrix} C_H \\ C_D \end{bmatrix} = \frac{1}{(T_{H1}\cdot T_{D2} - T_{D1}\cdot T_{H2})} \begin{bmatrix} T_{D2}\cdot S_1 - T_{D1}\cdot S_2 \\ -T_{H2}\cdot S_1 + T_{H1}\cdot S_2 \end{bmatrix} \tag{12}$$

$$= \frac{1}{\det} \begin{bmatrix} (T_{D2}\cdot \xi\cdot u_1\cdot t_1 - T_{D1}\cdot \xi\cdot u_2\cdot t_2) \pm \sqrt{T_{D2}\cdot(\xi\cdot u_1\cdot t_1) + T_{D1}\cdot(\xi\cdot u_2\cdot t_2)} \\ (-T_{H2}\cdot \xi\cdot u_1\cdot t_1 + T_{H1}\cdot \xi\cdot u_2\cdot t_2) \pm \sqrt{T_{H2}\cdot(\xi\cdot u_1\cdot t_1) + T_{H1}\cdot(\xi\cdot u_2\cdot t_2)} \end{bmatrix} \tag{13}$$

where the signal $S_1(S_2)=\xi\cdot u_1(u_2)\cdot t_1(t_2)$, $u_1=T_{H1}\cdot u_H+T_{D1}\cdot u_D$ and $u_2=T_{H2}\cdot u_H + T_{D2}\cdot u_D$, $\det=T_{H1}\cdot T_{D2}-T_{D1}\cdot T_{H2}$, u_H is the intensity of hydrogen, u_D is the intensity of deuterium, ξ is the photometrical sensitivity, and $t_1(t_2)$ is the measurement time of mode 1 (2). The signal-to-noise ratio (hereafter it is referred as *SNR*) can be given from the ratio of the expected signal and signal fluctuations as

$$SNR(D) = \frac{|-T_{H2}\cdot \xi\cdot u_1\cdot t_1 + T_{H1}\cdot \xi\cdot u_2\cdot t_2|}{\sqrt{T_{H2}\cdot \xi\cdot u_1\cdot t_1 + T_{H1}\cdot \xi\cdot u_2\cdot t_2}} \tag{14}$$

$$= \frac{\sqrt{\xi}\cdot|(T_{H1}\cdot T_{D2} - T_{H2}\cdot T_{D1})\cdot u_D|}{\sqrt{T_{H2}\cdot T_{H1}\cdot u_H + T_{H2}\cdot T_{D1}\cdot u_D + T_{H1}\cdot T_{H2}\cdot u_H + T_{H1}\cdot T_{D2}\cdot u_D}}\sqrt{t} \tag{15}$$

Under an ideal condition that $T_{H1}=1.0$, $T_{D1}=1.0$ in equation (15) and assuming that $t_1=t_2=t$, the *SNR* of the deuterium signal can be reduced as

$$SNR(D) = \frac{\sqrt{\xi}\cdot|(T_D - T_H)\cdot u_D|}{\sqrt{2\,T_{H2}\cdot u_H + T_{H2}\cdot T_{D1}\cdot u_D + T_{D2}\cdot u_D}}\sqrt{t} \tag{16}$$

$$\sim \frac{|(T_D - T_H)\cdot u_D|}{\sqrt{2\,T_H\cdot u_H}}\sqrt{\xi\cdot t} \tag{17}$$

($\because$ the intensity of hydrogen $u_H \gg$ the intensity of deuterium u_D)

From equation (17), it is found that the *SNR* of deuterium measurement is proportional to the square root of the measurement time, and the ratio is related to the transmission of the hydrogen absorption cell.

3 Application to imaging observations of the Martian hydrogen and deuterium corona

As an initial step to retrieve the Martian D/H ratio, images of the Martian corona are simulated. The Lyman α intensity of the Martian hydrogen and deuterium corona is calculated. The model considers a resonance scattering process in the Martian coronas by Monte Carlo simulation. Note that this model was originally developed for an analysis of geocorona (Ito, 2001). In the model, the atomic hydrogen density distribution is assumed as the same profile obtained by the Mariner Series (Anderson *et al.*, 1971, 1974). The atomic deuterium density is assumed by multiplying a factor 9×10^{-4} to the hydrogen model, which gives a good approximation to the nadir or bright limb. The temperature of the corona is assumed to be 350 K for both hydrogen and deuterium coronas. No CO_2 atmosphere is assumed. The position of Nozomi spacecraft is

assumed to be located at (0, $-2R_M$, 0) in Mars-Sun-equatorial coordinates. False-color maps of Lyman α emissions of hydrogen and deuterium are shown in Figs. 3(a) and (b). The maximum intensities of the hydrogen and deuterium corona are simulated as ~5,000 [R] and ~25 [R], respectively.

By substituting all parameters listed in Table 1 into equation (17), 3D-distribution of the *SNR* of the deuterium corona can be obtained as shown in Fig. 4. It is found that the *SNR* of deuterium corona observation for one hour is ~0.4 at maximum. We have also calculated the averaged intensity of the hydrogen and deuterium Lyman α emissions

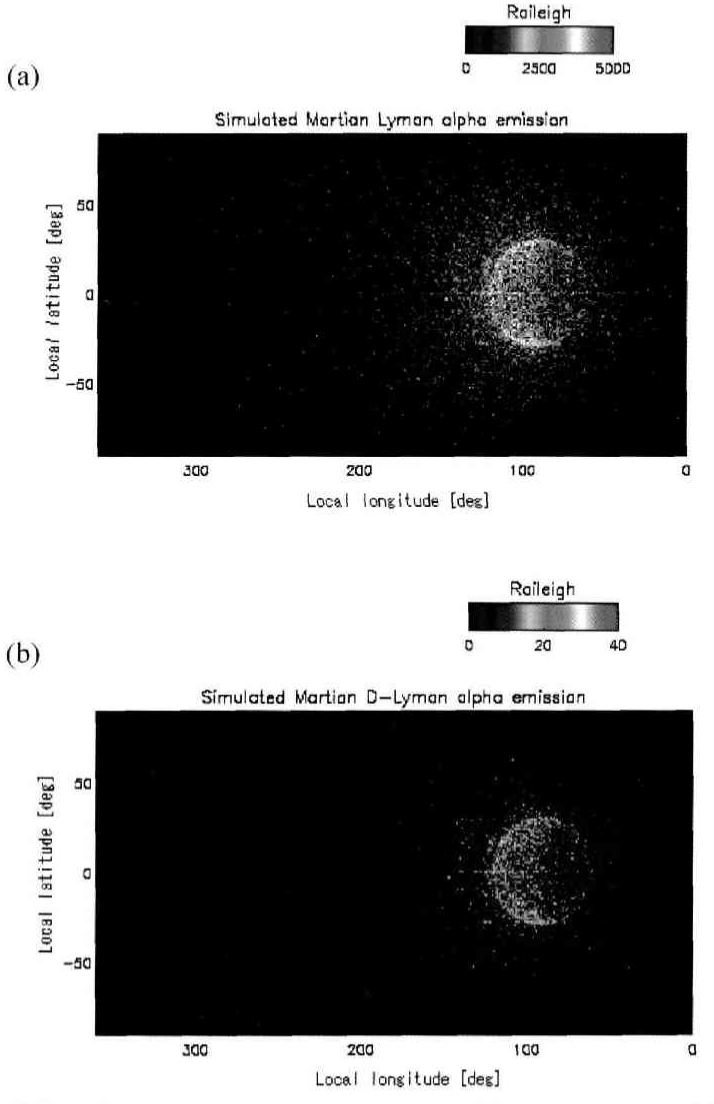

Fig. 3. False-color plots of the Martian hydrogen and deuterium corona. (a) The hydrogen corona with a brightest limb intensity of ~5,000 [R], and (b) the deuterium corona with a brightest limb intensity of ~25 [R].

Table 1. List of parameters used for this simulation.

Items	Values
Sensitivity (P_S)	2.83×10^{-3} [cps/R]
Integration time (IT)	3,600 [sec]
Nozomi position (x, y, z)	(0, $-2\ R_M$, 0)
Transmission of hydrogen (T_H)	0.6
Tranmission of deuterium (T_D)	0.9

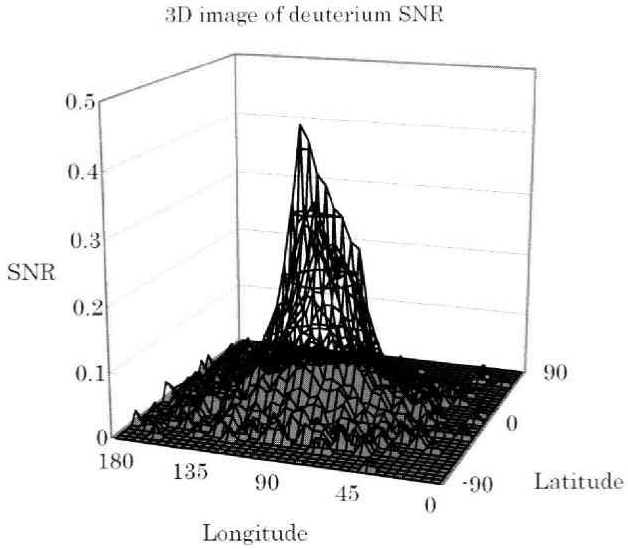

Fig. 4. Three-dimensional display of the SNR per 1 hour in the case of deuterium corona measurement with $T_H=0.6$ and $T_D=0.9$.

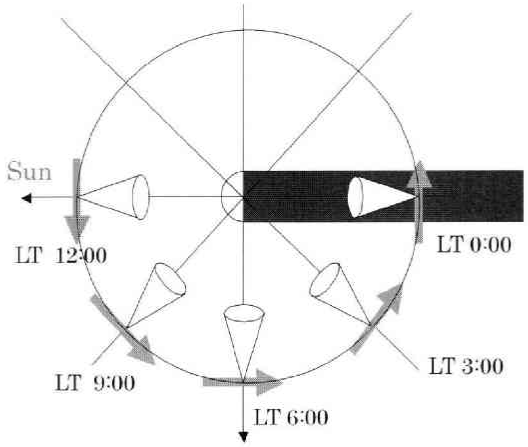

Fig. 5. Schematic diagram of the NOZOMI spacecraft location.

at 25 positions around Mars as shown in Fig. 5. The distance of the Nozomi spacecraft from the center of the Mars is given as 1.044 R_M (150 km altitude), 2 R_M, 5 R_M, 10 R_M and 15 R_M, while the local time of the spacecraft is given as 0, 3, 6, 9 and 12 hours, respectively. The averaged scattering intensities of the H and D Lyman α emissions are obtained by averaging the whole Lyman α emissions inside the disk direction. The result is summarized in Table 2. The averaged hydrogen and deuterium Lyman α emissions obtained from our Monte Carlo simulations are ~5,600 [R] and ~28 [R] at the dayside periapsis (1.044 R_M), respectively, while they are ~205 [R] and ~1 [R] at the nightside apoapsis (15 R_M).

4 Application to the remote sensing of the D/H ratio in the Martian Corona

In order to accurately estimate the *SNR* of the D/H ratio from the actual observation of the Martian corona, we must consider actual background intensity and dark noise. However, under the present simple condition that the corona is pure hydrogen and deuterium gases, the *SNR* of D/H ratio can be expressed as

$$SNR(\mathrm{D/H}) \sim SNR(\mathrm{D}) \tag{19}$$

Consequently, the *SNR* of the D/H ratio can be estimated by the *SNR* of the deuterium signal.

Imaging observations of the Martian hydrogen and deuterium corona are performed by the spin scan and orbital motion of the Nozomi spacecraft as shown in Fig. 6. The *SNR* of the D/H ratio can be estimated from equation (17) using the averaged intensity of hydrogen and deuterium corona listed in Table 2 as well as the orbital information of the spacecraft. The result is summarized in Table 3. Note that the periapsis is 1.044

Table 2. Averaged intensities (Rayleigh) of hydrogen and deuterium Lyman α scattering emissions viewed from 25 positions around Mars.

	Distance	1.044 R_M	2 R_M	5 R_M	10 R_M	15 R_M
	AD[1]	146.5°	60.0°	19.2°	10.4°	7.2°
H	12 : 00	5,810	2,856	1,405	1,188	1,114
	9 : 00	4,830	2,522	1,282	1,080	1,011
	6 : 00	3,469	1,744	847	697	660
	3 : 00	2,142	970	398	329	307
	0 : 00	1,110	582	263	218	205
D	12 : 00	28.0	13.8	6.8	5.7	5.4
	9 : 00	23.3	12.2	6.2	4.9	4.9
	6 : 00	16.7	8.4	4.1	3.4	3.2
	3 : 00	10.3	4.7	1.9	1.6	1.5
	0 : 00	5.4	2.8	1.3	1.1	1.0

[1] AD denotes Angle Diameter of the Martian disk from an assumed altitude of the Nozomi spacecraft.

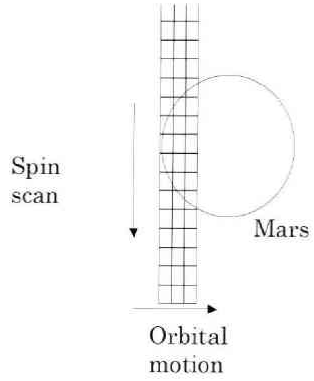

Fig. 6. Schematic diagram of the spin scan orbital motion method.

Table 3. Estimated *SNR* of the deuterium Lyman α measurement at different locations of the Nozomi spacecraft.

Altitude / LT	0.044 R_M (150 km)	1 R_M	2 R_M	5 R_M	15 R_M
12 : 00	1.969	3.115	2.806	2.215	1.621
9 : 00	1.384	2.257	1.991	1.502	1.161
6 : 00	0.972	1.609	1.394	0.948	0.802
3 : 00	0.886	1.385	1.274	0.878	0.745
0 : 00	0.867	1.432	1.233	0.852	0.698

R_M distance (150 km altitude), and the apoapsis is 15 R_M distance, while the orbital period is 38 hours. The observation time t_{obs} is estimated by the time for scanning the Martian disk as

$$T_{obs} = 3397/\text{velocity} \cdot (\pi/4 \sin(\Omega/2)) \tag{20}$$

For example, in case that the Nozomi spacecraft is located at an altitude of 1 R_M, the *SNR* of the D/H ratio can be estimated as $\sim$3.1. From this estimation, it is concluded that the D/H absorption cell photometer has sufficient instrumental performance.

5 Summary

In this paper, we summarize the performance of the developed D/H absorption cell photometer on board the Nozomi spacecraft and the results of simulation studies on D/H ratio retrieval from Martian corona measurement. The developed cell has sufficient instrumental performance and thereby contributes to the measurement of the D/H ratio in the Martian corona. The major results obtained in this study are summarized as follows.

1. A D/H absorption cell has been developed for the Nozomi spacecraft. By

measuring the absorption cell profiles, we have obtained quantitative parameters such as optical depth and kinetic temperature to characterize the absorption cell profile.

2. A hydrogen/deuterium Lyman α scattering property has been calculated using Monte Carlo simulation and a radiative transfer equation. The maximum intensities of the hydrogen and deuterium Lyman α emissions have been estimated as ~5,000 [R] and ~25 [R], respectively.
3. Imaging observations of hydrogen/deuterium corona and the retrieval of the Martian D/H ratio from the observation data have been investigated. In case that the transmission ratios of the hydrogen and deuterium Lyman α emissions are 0.5 and 0.9, respectively, the *SNR* of globally averaged D/H ratio is estimated to be ~2.0 at 150 km altitude. The estimated *SNR* demonstrates that the D/H absorption cell photometer has good enough performance to retrieve the Martian D/H ratio.

Acknowledgments

The authors thank to the NOZOMI/UVS team members for providing us various testing data.

References

Anderson D.E. Jr., 1974 : Mariner 6, 7, and 9 ultraviolet spectrometer experiment : Analysis of hydrogen Lyman α data, *J. Geophys. Res.*, **79**, 1513-1518.

Anderson D.E. Jr. and C.W. Hord., 1972 : Correction to "Mariner 6 and 7 ultraviolet spectrometer experiment : analysis of hydrogen Lyman α data, *J. Geophys. Res.*, **76**, 6666, 1971", *J. Geophys. Res.*, **77**, 5638.

Bertaux, J.L. and F. Montmessin, 2001 : Isotopic fractionation through water vapor condensation : The deuteropause, a cold trap for deuterium in the atmosphere of Mars, *J. Geophys. Res.*, **106**, 32879-32884.

Bjoraker, G.L., M.J. Mumma, and H.P. Larson, 1989 : Isotopic abundance ratios for hydrogen and oxygen in the Martian atmosphere, *Bull. Am. Astron. Soc.* **21**, 991.

Carr, M.H., 1979 : Formation of Martian flood features by release of water from confined aquifers, *Geophys. Res.* **84**, 2995-3007.

Carr, M.H., 1986 : Mars : A water-rich planet ?, *Icarus*, **68**, 187-216.

Carr, M.H., 1987 : Water on Mars, *Nature*, **326**, 30-35.

Carr, M.H., 1990 : D/H on Mars : Effects of floods, volcanism, impacts, and polar processes, *Icarus*, **87**, 210-227.

Chamberlain, J.W., 1069 : Escape rate of hydrogen from a carbon dioxiode atmosphere, *Asrtrophys. J.* **155**, 711-714.

Cheng, B., E.P. Chew, C. Liu, M. Bahou, Y. Lee, Y.L. Yung, and M.F. Gerstell, 1999 : Photo-induced fractionation of water isotopomers in the Martian atmosphere, *Geophys. Res. Lett*, **26**, 3657-3660.

Esposito, L.W., J.E. Colwell, and W.E. McClintock, 1998 : Cassini UVIS observations of Saturn's rings, *Planet. Space Sci.*, **46**, 1221-1235.

Formisano, V., D. Grassi, N. Ignatiev, L. Zasova, and A. Maturilli, 2002 : PFS for Mars Express : A new approach to study Martian atmosphere, *Adv. Space Res.*, **29**, 131-142.

Fouchet, T. and E. Lellouch, 2000 : Vapor pressure isotope fractionation effects in planetary atmo-

spheres : Application to deuterium, *Icarus*, **144**, 114-123.
Fox, J.L., 1993 : On the escape of oxygen and hydrogen from Mars, *J. Geophys. Res.*, **20**, 1747-1750.
Fukunishi, H., S. Watanabe, M. Taguchi, S. Okano, and Y. Takahashi, 1999 : Mars ultraviolet imaging spectrometer experiment on the Planet-B mission, *Adv. Space Res.*, **23**, 1903-1906.
Hunten, D.M., 1982 : Thermal and nonthermal escape mechanisms for terrestrial bodies, *Planet. Space Sci.*, **30**, 773-783.
Hunten, D.M., 1990 : Kuiper prize lecture : escape of atmosphere, ancient and modern, *Icarus*, **85**, 1-20.
Ito, K., T. Namioka, Y. Morioka, T. Sasaki, H. Noda, K. Goto, T. Katayama, and M. Koike, 1986 : High resolution VUV spectroscopic facility at the photon factory, *Appl. Opt.*, **25**, 837-847.
Ito, Y., 2001 : Remote sensing of the geocorona on board the NOZOMI spacecraft. Doctoral thesis, Tohoku University.
Korablev, O.I, M. Ackerman, V.A. Krasnopolsky, V.I. Moroz, C. Muller, A.V. Rodin, and S.K. Atreya, 1993 : Tentative identification of formaldehyde in the Martian atmosphere, *Planet. Space Sci.*, **41**, 441-451.
Krasnopolsky, V.A., M.J. Mumma, and G. Randall, 1998 : Detection of atomic deuterium in the upper atmosphere of Mars, *Science*, **280**, 1576-1580.
Krasnopolsky, V.A., 2000 : On the deuterium abundance on Mars and some related problems, *Icarus*, **148**, 597-602.
Liu, S.C. and T.M. Donahue, 1976 : The regulation of hydrogen and oxygen escape from Mars, *Icarus*, **28**, 231-246.
Owen, T., J.P. Maillard, C.L. de Bergh, and L. Barry, 1988 : Deuterium on Mars : the abundance of DO and the value of D/H, *Science*, **240**, 1767-1770.
Taguchi, M., H. Fukunishi, S. Watanabe, S. Okano, Y. Takahashi, and T.D. Kawahara, 2000a : Ultraviolet imaging spectrometer (UVS) experiment on board the NOZOMI spacecraft : Instrumentation and initial results, *Earth Planets Space*, **52**, 49-60.
Taguchi, M., G. Funabashi, S. Watanabe, Y. Takahashi, and H. Fukunishi, 2000b : Lunar albedo at hydrogen Lyman α by the NOZOMI/UVS, *Earth Planets Space*, **52**, 645-647.
Tsuruda, K., I. Nakatani, and T. Yamamoto, 1996 : PLANET-B mission to Mars-1998, *Adv. Space Res.*, **17**, 21-29.
Visconti, G., 1977 : Hydrogen escape in the terrestrial atmosphere at low oxygen levels : A photochemical model, *J. Atmos. Sci.*, **34**, 193-204.
Watson, L.L., I.D. Hutcheon, S. Epstein, and E.M. Stolper, 1993 : D/H ratios and water contents of Amphiboles in magmatic inclusions in Chassigny and Shergotty, *Meteoritics*, **28**, 456.
Yung, Y.L., J. Wen, J.P. Pinto, K.K. Pierce, and M. Allen, 1988 : HDO in the Martian atmosphere-Implications for the abundance of crustal water, *Icarus*, **76**, 146-159.
Yung, Y.L. and D.M. Kass, 1998 : Deuteronomy ? : A puzzle of deuterium and oxygen on Mars, *Science*, **280**, 1545-1946.
Zahnle, K.J. and J.F. Kasting, 1986 : Mass fractionation during transonic escape and implications for loss of water from Mars and Venus, *Icarus*, **68**, 462-480.

Appendix

Calibration of the absorption cells using the 6VOPE spectrometer

As pointed out in Section 2, it is essential to understand the absorption cell property in order to correctly retrieve the kinetic temperature of incident Lyman α emission. In order to quantitatively measure the absorption cell property, we have used a VUV spectrometer facilitated at Tukuba High Energy Particle Laboratory. This spectrometer is called 6VOPE (6.65-m vertical dispersion off-plane eagle spectrometer) (Ito *et al.*, 1986). Optical setup for calibration of the absorption cell at 6VOPE is shown in Fig. A1. We have measured the absorption cell profiles. Examples of measured absorption profiles and fitted profiles are shown in Figs. A2(a) and (b) for the hydrogen and deuterium cells. By performing least square fitting of a Gaussian function to the measured profile, we have successfully obtained unique parameters : kinetic temperature (T_{atom}) of hydrogen (deuterium) atoms and the optical depth (τ_0) which identify the absorption cell profiles.

The relationship between the atomic temperature and the filament power consumption of the hydrogen and deuterium cells are summarized in Figs. A3(a) and (b). Also, the relationship between the optical depth and the filament power consumption of the hydrogen and deuterium cells are summarized in Figs. A4(a) and (b). The atomic hydrogen gas temperature T_H and the optical depth τ_H of the hydrogen absorption cell are given as

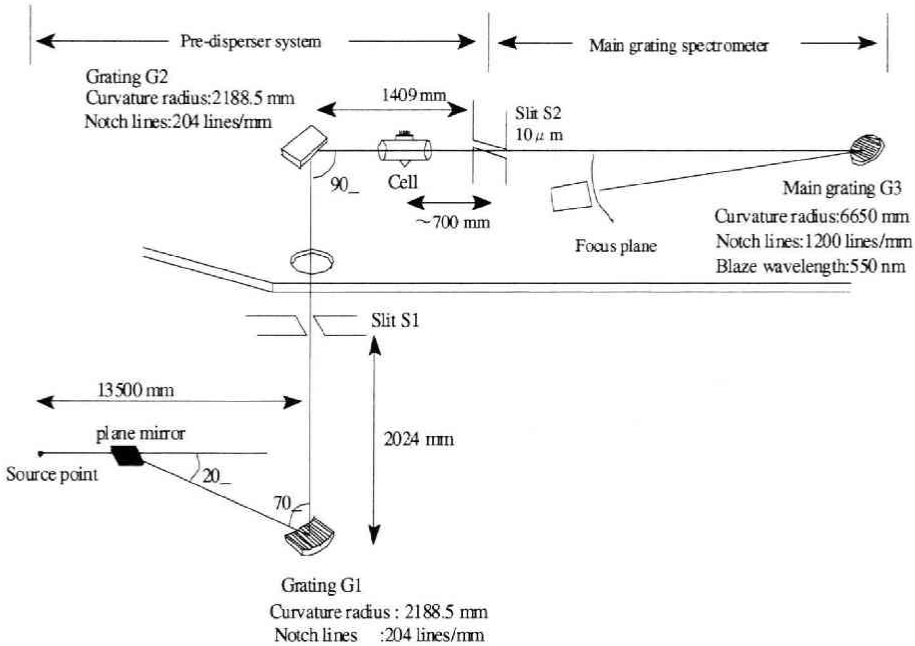

Fig. A1. Layout of the absorption profile measurement of the cell using the 6VOPE spectrometer.

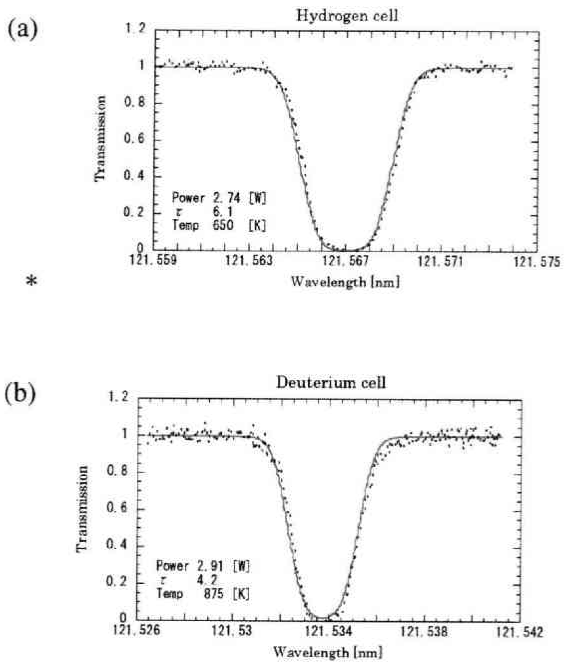

Fig. A2. Examples of absorption profile measurements and fitted Gaussian curves for the hydrogen cell (a) and the deuterium Lyman cell (b).

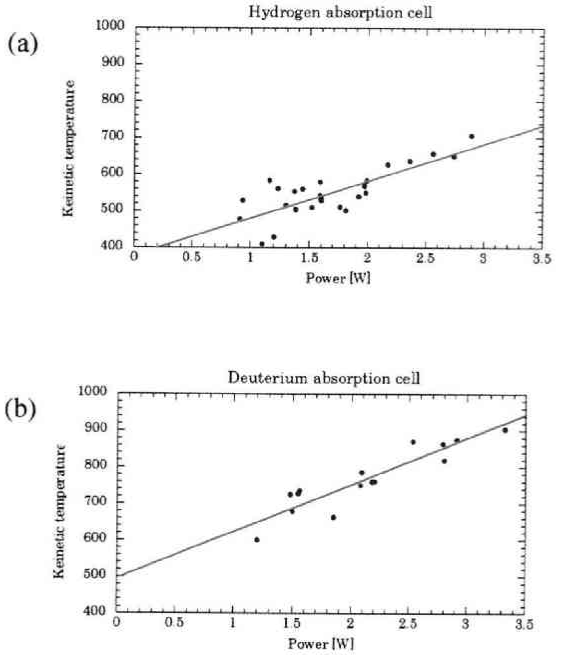

Fig. A3. Variations in the kinetic temperature of atomic gas in the cell as a function of filament power consumption and a least square fitting to them, for the hydrogen cell (a) and the deuterium cell (b).

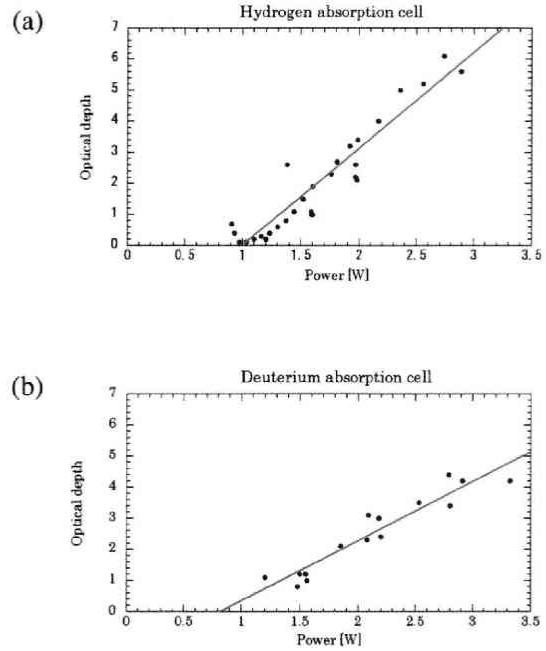

Fig. A4. Variations in the optical depth of the absorption cell as a function of filament power consumption and a least square fitting to them, for the hydrogen cell (a) and the deuterium cell (b).

$$T_H = 101 \times P + 381 \tag{A1}$$

$$\tau_H = 3.1 \times P - 3.1 \tag{A2}$$

where P [W] is the filament power consumption. The atomic deuterium gas temperature T_D and the optical depth τ_D of the deuterium absorption cell are given as

$$T_D = 126 \times P + 499 \tag{A3}$$

$$\tau_D = 1.9 \times P - 1.6 \tag{A4}$$

The values of τ_H and τ_D are assumed to be zero in the range in which these values become negative. From these fitting results, we have quantitatively evaluated the performance of the absorption cell.